Calmodulin Mediates DNA Repair Pathways Involving H2AX in Response to Low-Dose Radiation Exposure of RAW 264.7 Macrophages

ARTICLE *in* CHEMICAL RESEARCH IN TOXICOLOGY · MARCH 2009

Impact Factor: 3.53 · DOI: 10.1021/tx800236r · Source: PubMed

5 AUTHORS, INCLUDING:

Heather S Smallwood
The University of Tennessee Health Scienc…
20 PUBLICATIONS **446** CITATIONS
SEE PROFILE

Daniel Lopez-Ferrer
Caprion
33 PUBLICATIONS **1,371** CITATIONS
SEE PROFILE

Calmodulin Mediates DNA Repair Pathways Involving H2AX in Response to Low-Dose Radiation Exposure of RAW 264.7 Macrophages

Heather S. Smallwood,* Daniel Lopez-Ferrer, P. Elis Eberlein, David J. Watson, and Thomas C. Squier

Washington State University Tri-Cities, Richland, Washington 99352, and Cell Biology and Biochemistry Group, Biological Sciences Division, Pacific Northwest National Laboratory, Richland, Washington 99352

Received June 27, 2008

Understanding the molecular mechanisms that modulate macrophage radioresistance is necessary for the development of effective radiation therapies, as tumor-associated macrophages promote both angiogenesis and matrix remodeling that, in turn, enhance tumor metastasis. In this respect, we have identified a dose-dependent increase in the abundance (i.e., expression level) of the calcium regulatory protein calmodulin (CaM) in RAW 264.7 macrophages upon irradiation. At low doses of irradiation there are minimal changes in the abundance of other cellular proteins detected using mass spectrometry, indicating that increases in CaM levels are part of a specific radiation-dependent cellular response. CaM overexpression results in increased macrophage survival following radiation exposure, acting to diminish the sensitivity to low-dose radiation exposures. Following macrophage irradiation, increases in CaM abundance also result in an increase in the number of phosphorylated histone H2AX foci, associated with DNA repair, with no change in the extent of double-stranded DNA damage. In comparison, when nuclear factor κB (NFκB)-dependent pathways are inhibited, through the expression of a dominant-negative IκB construct, there is no significant increase in phosphorylated histone H2AX foci upon irradiation. These results indicate that the molecular basis for the up-regulation of histone H2AX-mediated DNA repair pathways is not the result of nonspecific NFκB-dependent pathways or a specific threshold of DNA damage. Rather, increases in CaM abundance act to minimize the low-dose hypersensitivity to radiation by enhancing macrophage radioresistance through processes that include the up-regulation of DNA repair pathways involving histone H2AX phosphorylation.

Introduction

As part of the innate immune system, macrophages are phagocytic cells that represent a first line of defense that recognize aberrant cells for clearance. In the presence of solid tumors, paracrine signaling mechanisms act to reprogram macrophages in such a way that pathways associated with the oxidative burst are disrupted (*1*). Moreover, these tumor-associated macrophages release inflammatory cytokines such as tumor necrosis factor α (TNFα)[1] and matrix metalloproteases that promote angiogenesis and matrix remodeling to enhance tumor survival (*2*). For these reasons, tumor-associated macrophages are considered indicators of tumor progression and invasiveness and represent important targets for therapeutic interventions in conjunction with normal radiation therapies. One complication of radiation treatment is the significant radioresistance of macrophages relative to malignant tumor cells (*3*). In this respect, current therapeutic treatments seek to exploit sensitive pathways that enhance macrophage killing in tumors. For example, radiotherapies that combine pharmaceuticals that target inflammatory responses involving NFκB nuclear activation can enhance the ability to kill some tumors (*4*).

Cell killing in response to radiation exposure is biphasic due to a low-dose hypersensitivity exhibited by most cells. Radiation hypersensitivity is thought to represent the inability of cells to detect DNA damage below a finite threshold, thus minimizing the activation of error-prone repair systems in the absence of substantive DNA damage (*5*). Depending on the radiation dose, different cellular effects are observed. Low-dose radiation treatments have a pronounced anti-inflammatory effect on macrophages; in contrast, high doses of radiation are pro-inflammatory, resulting in the expression of cytokines (e.g., TNFα) following the activation of NFκB (*6*). One such regulatory protein modulated through macrophage activation pathways involving NFκB is calmodulin (CaM) (*7*); alterations in the abundance of CaM can result in large changes in cellular function through the modulation of CaM-dependent pathways (*8, 9*). This is especially relevant, as increases in CaM abundance have been reported in response to radiation exposures in epidermal tissues and submandibular salivary glands (*10, 11*). While the consequences of radiation-induced increases in CaM abundance are unclear, prior measurements have reported CaM to be part of a dynamic complex with histone H2AX. Histone H2AX specifically associates with chromatin and is phosphorylated at exposed double-stranded DNA breaks in euchromatin

* To whom correspondence should be addressed at St. Jude Children's Research Hospital. Phone: (901) 595-2353. Fax: (901) 595-3107. E-mail: Heather.Smallwood@StJude.org.

[1] Abbreviations: CaM, calmodulin; EGTA, ethylene glycol bis(β-aminoethyl ether)-*N*,*N*,*N*′,*N*′-tetraacetic acid; FBS, fetal bovine serum; γH2AX, histone H2AX phosphorylated at Ser-139; HRP, horseradish peroxidase; IκB, inhibitor of NFκB; IκBαM, dominant-negative mutant of IκB in which phosphorylation sites for IκB kinase are mutated (i.e., S32A and S36A); IFNγ, interferon γ; iNOS, inducible nitric oxide synthase; LPS, lipopolysaccharide; NFκB, nuclear factor κB; PBS, phosphate-buffered saline; ROS, reactive oxygen species; SDS−PAGE, sodium dodecyl sulfate−polyacrylamide gel electrophoresis; Sp1, specificity protein 1; TNFα, tumor necrosis factor α.

10.1021/tx800236r CCC: $40.75
Published on Web 02/05/2009

to promote DNA repair, through the recruitment of a supramolecular protein complex (*12*−*15*). DNA breaks are associated with either cell killing or transformation (*16*). Thus, to develop effective radiotherapies, an understanding of the functional linkages between NFκB activation, CaM abundance, and alterations in DNA repair pathways and their effects on the radiosensitivity of macrophages is needed.

To understand the mechanisms that contribute to the radioresistance of macrophages, and the possible roles of NFκB- and CaM-dependent signaling pathways in radioresistance, we have investigated how the selective modulation of these pathways affects cell survival following irradiation. Complementary measurements assess changes in total cellular protein abundances, DNA damage, the activation of associated DNA repair pathways involving histone H2AX, and their relationship to macrophage survival. Measurements were made using wild-type RAW 264.7 macrophages or constructs in which (i) CaM is overexpressed by 2-fold or (ii) NFκB-dependent inflammatory pathways are selectively inhibited following expression of a dominant-negative mutant of IκBα (i.e., IκBM), where this construct is deficient in critical phosphorylation sites necessary for the release of inhibition (*7*). We report that increasing radiation exposure results in dose-dependent increases in CaM abundance, with minimal changes in the abundance of other proteins detected by mass spectrometry. An increase in CaM abundance is functionally important, as macrophages that overexpress CaM exhibit enhanced macrophage survival in response to radiation. This increase in radioresistance is mediated through the activation of CaM-dependent DNA repair pathways involving phosphorylated histone H2AX, which is shown to be mechanistically distinct from DNA damage accumulation and classical NFκB-dependent proapoptotic pathways. The latter result is consistent with recent reports that indicate the activation of cellular DNA damage response pathways does not require DNA damage (*17*).

Experimental Procedures

Materials. Ampicillin, RPMI 1640 medium (no. 0030078DJ), fetal bovine serum (FBS), penicillin, streptomycin, and G418 were from Gibco (Carlsbad, CA). Antibodies used include a polyclonal antibody against full-length CaM (sc-5537, Santa Cruz Biotechnology, Inc., Santa Cruz, CA) and a rabbit polyclonal antibody against phosphorylated Ser-139 in histone H2AX (i.e., γH2AX) (Calbiochem Inc., San Diego, CA). Wild-type RAW 264.7 murine macrophages and stably transfected constructs were generated as previously described (*7*), which express either (i) a 2-fold molar excess of CaM cloned into a pcDNA3.1 vector (Invitrogen Inc., Carlsbad, CA) (i.e., RAW−CaM) or (ii) a dominant-negative construct of IκBα cloned into a pCMV vector (BD Bioscience, Sparks, MD) (i.e., RAW−IκBM) whose phosphorylation sites for IκB kinase were mutated (i.e., S32A and S36A) to block NFκB activation. Stable transfectants were maintained in RPMI medium supplemented with G418 as the selection agent to maintain plasmids pcDNA3.1 and pCMV.

Cell Culture and Radiation Exposure. RAW 264.7 macrophages were grown to ~70% confluency in RPMI 1640 medium supplemented with 10% heat-inactivated FBS and a 1% mixture of penicillin and streptomycin (both at 1%, v/v) in a humidified atmosphere of 5% CO_2 and 95% air at 37 °C. Growth rates were equivalent for all cells (i.e., WT, CaM, and IκBM) (*7*). All cell lines were each passaged three times per week, and total cell passages were kept below 40 for all experiments. Prior to irradiation, freshly plated cells were incubated overnight. The cells were irradiated using X-ray or ^{60}Co sources at calibrated dose rates ranging from 0.1 to 0.6 Gy/min for dose response curves and 0.33 Gy/min for single 1 Gy dose exposures.

Cellular Survival Assays. Cells were irradiated for 1 h following seeding of macrophages on 100 mm diameter tissue culture plates at a density of 200 or 500 cells per plate. Colonies were counted after one week following fixation and Giemsa staining, essentially as previously described (*18*). The plating efficiency was calculated as the fraction of colonies per seeded cell surviving in untreated (sham) controls, and in all cases the fraction of surviving cells following irradiation was corrected by the plating efficiency. Alternatively, the viability of individual cells was determined 1 h following irradiation for macrophages grown in 24-well Sensorplate coverslip plates (Greiner Bio-One Inc., Monroe, NC) by comparing the fluorescence signal increases upon DNA intercalation of propidium iodide (1 μM) (which is impermeable to live cells and thus selectively detects dead cells) and Hoeschst 33342 (1 μM) (which is cell-permeable and recognizes all cells). Images were captured using a Nikon Eclipse TE300 epifluorescence microscope; live and apoptotic cells were automatically located on the basis of condensation of Hoechst-stained nuclei using Volocity high-performance imaging software (Improvision Inc., Waltham, MA). The identification of condensed nuclei by morphological characterization using microscopy represents the "gold standard" for accurately identifying apoptotic cells (*19*−*23*). Combined with automated analysis methods, experimental bias is avoided to accurately identify cells that have committed to cellular apoptosis (*24*). In this respect, Hoechst 33342 preferentially binds to double-stranded DNA, and is "often used to distinguish condensed pycnotic nuclei in apoptotic cells" (http://www.biocompare.com/details/246550/Hoechst-33342-trihydrochloride-trihydrate-from-Molecular-Probes-(Invitrogen).html), where apoptosis is associated with an apoptotic cascade that culminates in chromatin condensation (pyknosis) and DNA fragmentation.

DNA Damage. Double-stranded DNA breaks were assessed using the CometAssay HT kit from Trevigen (Gaithersburg, MD), which employs the neutral Comet assay. The Comet assay detects the majority of apurinic sites, apyrimidinic sites, and alkali-labile DNA adducts (e.g., phosphoglycols and phosphotriesters) (http://www.trevigen.com/). The neutral Comet assay involves an alkaline lysis of labile DNA at sites of damage followed by separation under neutral conditions [i.e., in Tris-buffered EDTA (TBE solution), as previously described by Yashuahara and co-workers] to permit the selective detection of double-stranded DNA breaks (*25*). All procedures were carried out in the dark as previously described (*26*). Briefly, irradiated cells were harvested and incubated with agarose on slides for 20 min prior to immersion in ice cold lysis buffer for 45 min. The slides were then sequentially (i) transferred to an alkaline solution (i.e., 300 mM NaOH and 200 mM EDTA) for 40 min, (ii) subjected to horizontal electrophoresis for 10 min at 1 V/cm in the supplied Tris-buffered EGTA (TBE) (permitting the selective detection of double-stranded DNA breaks), and (iii) fixed in ethanol for 5 min and air-dried. DNA was stained with SYBER Green I, which selectively detects double-stranded DNA, and fluorescence was imaged in the presence of Prolong Gold antifade mounting medium (Molecular Probes) using a Nikon Eclipse TE300 epifluorescence microscope. Analysis of double-stranded DNA breaks was based on the increased mobility of the DNA "tail length" in the electric field and was quantified by close-fitting segmentation as previously described by Vilhar and co-workers (http://botanika.biologija.org/exp/comet/Comet-principles.pdf) using Volocity high-performance imaging software.

DNA Repair Pathways. Central to the recruitment of the two well-known pathways associated with the repair of double-stranded DNA (i.e., nonhomologous end-joining and homologous recombination) is the phosphorylation of H2AX (to form γ-H2AX) in association with chromatin, where γ-H2AX acts to promote the recruitment of DNA repair proteins (*13*). While most repair proteins that act on double-stranded DNA breaks appear to function exclusively in nonhomologous end-joining (NHEJ) or homologous recombination repair (HR) pathways, a number of repair proteins have been demonstrated to participate in both pathways, including histone H2AX, the MRE11/RAD50/NBS1(XRS2) complex, BRCA1, PARP-1, RAD18, DNA-dependent protein kinase catalytic

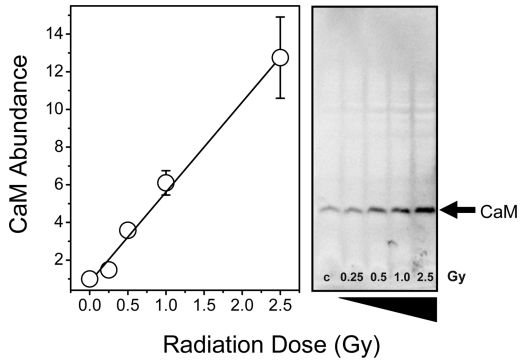

Figure 1. Radiation-dependent increases in CaM abundance. Western immunoblots against CaM (right) and densitometric analysis (left) of lysates (15 μg) from RAW 264.7 macrophages. Cells were harvested 2 h following irradiation and were lysed in 20 mM Tris (pH 8.0), 1% Nonidet P-40, 0.15 M NaCl, 1 mM Na_2PO_4, and 1 mM EGTA. Indicated values represent the average of two different measurements done in triplicate with associated standard deviations.

subunit (DNA-PKcs), and ATM (*27*). Accordingly, we have assessed the activation of central pathways involving repair of double-stranded DNA breaks through a consideration of histone H2AX. Foci associated with phosphorylated histone H2AX (γH2AX) in association with double-stranded DNA breaks on chromatin were imaged using immunofluorescence microscopy, essentially as previously described (*28*). Briefly, rinsed macrophages in PBS [137 mM NaCl, 2.7 mM KCl, 10 mM NaH_2PO_4 (pH 7.4)] were fixed using 4% paraformaldehyde in PBS, neutralized using NH_4Cl, permeabilized with 0.1% Triton X-100 in PBS, and incubated with a rabbit primary antibody against phosphorylated histone H2AX (i.e., γH2AXpSer139) (EMD Biosciences, Gibbstown, NJ) in the presence of 300 units of AlexaFluor568-labeled phalloidin (Molecular Probes Inc., Eugene, OR) to resolve the actin cytoskeleton. γH2AX was detected using the AlexaFluor488 goat antirabbit polyclonal antibody (Molecular Probes). The coverslips were then mounted upon microscope slides for analysis of DAPI-stained nuclei and imaged using Prolong Gold antifade mounting medium. Automated quantitation of the number of foci (larger than 0.05 μm^2) associated with γH2AX bound to chromatin within DAPI-stained nuclei used the Volocity high-performance imaging software.

Western Immunoblots. Abundance changes of the protein CaM were analyzed following cell lysis using immunoblots, as previously described (*7*). Briefly, protein concentrations of cellular lysates were determined by the Coomassie Plus Bradford reagent from Pierce (Rockford, IL) immediately after harvesting of the cells. Aliquots of equal protein were reduced with NuPAGE reducing agent, diluted into NuPAGE LDS sample buffer, and denatured by boiling for 5 min prior to the separation of proteins by electrophoresis using a 10% acrylamide NuPAGE Bis-Tris gel, where all reagents were from Invitrogen. The amount of total protein loaded onto this gel (15 μg) was carefully chosen to permit the visualization of the large increases in CaM abundance, maintaining the intensity of the individual bands in the linear region necessary for quantitative densitometry (*29*). In all cases the concentration of protein in the lysates was measured, and the same amount of protein was loaded in each lane (with a total protein variance of less than 10%). We emphasize that the variation in total protein loading was much less than the changes in CaM protein expression. After electroblotting onto 0.45 μm nitrocellulose membranes (Invitrogen) and blocking with 2% bovine serum albumin (Sigma Chemical Co., St. Louis, MO) in PBS (pH 7.4), the membranes were incubated with the indicated primary antibodies overnight at 4 °C, followed by incubation with the appropriate horseradish peroxidase (HRP)-conjugated secondary antibody. The proteins were subsequently detected using ECL plus from Amersham (Piscataway, NJ) and/or SuperSignal West Femtomax Sensitivity Substrate from Pierce. CaM abundance levels were quantified using densitometry, as we have previously described in detail (*29*).

Proteomic Analysis. Cellular extracts were denatured in 8 M urea, and the total protein content was determined using the Coomassie Plus assay (Pierce). Denatured proteins were processed as described previously using high intensity focused ultrasound (HIFU) (*30*). Briefly, proteins were reduced and alkylated in 25 mM ammonium bicarbonate (pH 8.25), 5 mM tris(carboxyethyl)phosphine (TCEP) and 50 mM iodoacetamide (IAA) by sonication for 3 min at 2% of the maximum ultrasound amplitude. Then, the samples were 4× diluted, trypsin was added (1:50, w/w), and the solutions were sonicated for 1 min. The resulting peptides were then acidified and prepared for mass spectrometric analysis using C_{18} solid-phase extraction (Supelco, Bellefonte, PA). Peptides were eluted from the column with 1 mL of 0.1% trifluoroacetic acid/80% acetonitrile and then lyophilized. For isotopic labeling, the resulting peptide samples were reconstituted in 25 mM ammonium bicarbonate with trypsin (1:20 protease to protein ratio) and dried again by vacuum centrifugation. The samples were then resuspended in 100 μL of either $H_2{}^{16}O$ or $H_2{}^{18}O$ (95%, Sigma-Aldrich) and sonicated for 5 min. Labeling was stopped by adding 1% formic acid. $^{16}O/^{18}O$ samples were then mixed (1:1 ratio) and analyzed using a capillary LC system coupled online with a hybrid LTQ-Orbitrap mass spectrometer (Thermo-Fisher, San Jose, CA) with an in-house developed ESI source, as described previously (*30*). Quantitation of peptide abundance was determined from LC−MS data sets through the identification of isotopically labeled pairs of identified peptides using our VIPER software (http://ncrr.pnl.gov/software/) (*31, 32*), and abundance ratios were calculated on the basis of the intensities of the peaks across the chromatographic peak, as previously described in detail (*30*). A histogram of the abundance ratios of identified peptides was fit to a normal distribution, and a standard two-tailed z test that takes into account a false discovery rate (FDR) of 10% was used to identify peptides whose abundance changes were statistically significant (*33*). Protein identifications required the detection of two unique peptide pairs.

Results

Increases in CaM Abundance in Response to Macrophage Radiation Exposure. To assess the effect of radiation exposure on CaM abundance in macrophages, cells were exposed to varying doses of γ irradiation, and abundance changes were measured using an antibody against CaM on Western immunoblots of cellular lysates. Following irradiation, RAW 264.7 macrophages were collected and lysed; anti-CaM immunoblots of the resulting lysates exhibit a single band migrating as a 17 kDa band (Figure 1). Linear dose-dependent increases in CaM abundance in macrophages result from exposure to increasing levels of ionizing radiation, with more than a 10-fold increase in CaM abundance following a 2.5 Gy exposure (Figure 1). Observed maximal increases in CaM abundance are observed 2 h following irradiation and persist for approximately 8 h (data not shown). Increases in CaM abundance in response to irradiation are consistent with earlier reports of large increases in CaM abundance in some tissues in response to high doses (10 Gy) of ionizing radiation (*10, 11*). However, the observed increases in CaM abundance in response to the lower radiation doses, used in the present study, suggest a possible role in mediating cellular response pathways to clinically relevant radiation doses.

CaM Abundance and Increased Macrophage Radioresistance. The radiation sensitivity of RAW 264.7 macrophages was measured using a well-established clonogenic survival assay (*18*). In wild-type cells a biphasic loss of cell viability associated with radiation dose is observed, where a hypersensitivity to radiation doses is observed below 0.5 Gy (Figure 2A). At higher radiation doses macrophages become less sensitive per unit dose (i.e., they become radioresistant) (Figure 2B). These results are consistent with prior observations

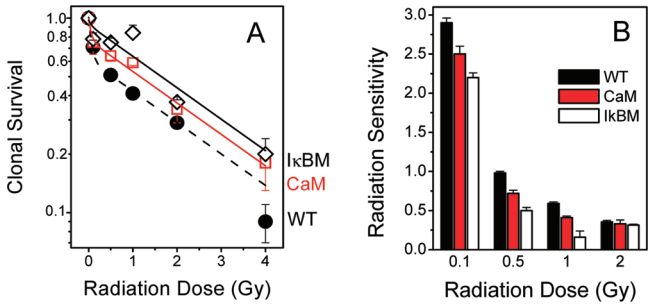

Figure 2. Increases in CaM abundance enhance clonal survival following radiation exposure. Clonal survival (*S*) (A) or radiation sensitivity [(1 − *S*)/radiation dose] (B) of macrophages plated following irradiation with indicated doses [wild-type RAW 264.7 macrophages (●, dashed line; black bar), stable cell lines overexpressing CaM (□, solid red line; red bar) or an IκB dominant-negative construct (IκBM) (◇, solid black line; open bar)] as described in the Experimental Procedures. Indicated values represent the average of six independent measurements and the associated standard errors of the mean. Lines represent least-squares fits to the following equation:

$$S = Ae^{-xD_\alpha} + (1-A)e^{-xD_\beta} \quad (1)$$

where D_α and D_β equal 0.06 ± 0.04 and 2.7 ± 0.3 Gy and represent low and high radiation doses associated with cellular killing for all cell types, and *A* is the fractional contribution associated with D_α, which for wild-type cells and constructs overexpressing CaM or IκBM, respectively, equals 0.38 ± 0.06, 0.23 ± 0.06, and 0.08 ± 0.06. Values of *A* for cells overexpressing CaM or IκBM are statistically different from that for wild-type cells ($p < 0.05$).

that different cellular mechanisms are associated with responses to low and high radiation doses in radioresistant cell lines (*34, 35*). The hypersensitivity associated with low-dose radiation has been suggested to indicate the requirement of a threshold level of DNA damage prior to the activation of repair pathways involving phosphorylated histone H2AX (i.e., γH2AX) (*5*). In view of prior proteomic measurements, demonstrating a radiation-sensitive association between CaM and histone H2AX in a transformed human embryonic kidney cell line (*12*), and our initial finding of a dose-dependent increase in CaM with irradiation, we have explored possible functional linkages between changes in CaM abundance and macrophage radioresistance.

A stable macrophage construct (i.e., CaM) was used that constitutively expresses a 2-fold higher abundance of CaM, mimicking the abundance changes observed following exposure to low doses (i.e., 0.25 Gy) of radiation (*7*). Overexpression of CaM results in no changes in cell cycle control or cellular morphology (Figure S4 in the Supporting Information) (*7*). Radiation-dependent increases in CaM abundance are blunted upon overexpression of CaM, where levels of CaM remain high and largely unchanged in response to cellular irradiation as is expected when the abundance of expressed proteins exceeds that of associated binding partners (*36*) (Figure S1A in the Supporting Information). These macrophages exhibit a significant (i.e., greater than 2-fold) increase in radioresistance as compared with wild-type controls, where the radiation dose necessary for 50% killing increases from 0.5 to 1.2 Gy (Figure 2A). Increases in CaM abundance selectively act to reduce the low-dose hypersensitivity to ionizing radiation, which is apparent at radiation doses of 0.5 Gy and below (Figure 2A). The radiation-dependent decrease in cell survival (i.e., slope) at higher radiation doses is independent of the overexpression of CaM (Figure 2). These results indicate that CaM acts to modulate the hypersensitivity of macrophages to low-dose radiation.

One transcription factor controlling CaM expression and other general inflammatory pathways in macrophages is NFκB (*7*). Thus, we have disrupted NFκB-dependent signaling through the expression of a dominant-negative IκB construct (IκBM) that lacks phosphorylation sites for IκB kinase. Following irradiation, we observe an increase in radioresistance upon expression of IκBM similar to that seen upon CaM overexpression (Figure 2). While inhibition of the NFκB pathway, through the expression of IκBM, results in decreases in CaM abundance levels (*7*), we observed an increase in CaM levels upon increasing levels of irradiation similar to, albeit blunted, that observed in wild-type cells (Figure S1A in the Supporting Information). These results suggest that increases in CaM levels upon irradiation do not involve NFκB-dependent pathways.

Consistent with this latter hypothesis, we find that cellular responses to low-dose radiation are very different from those associated with macrophage responses to bacterial lipopolysacharides, which result in substantial changes to the cellular proteome, including large increases in the abundance of iNOS through NFkB-dependent pathway activation (*7, 37*). In comparison, we detect no increases in iNOS abundance at low radiation doses (i.e., 1 Gy); increases in iNOS levels are only observed at higher doses of radiation (i.e., 2.5 Gy) (Figure S1B in the Supporting Information). Likewise, upon irradiation there are no detectable changes in the abundance of the cytokine TNFα, whose expression is CaM-dependent (*38*). These results indicate that increases in macrophage survival, upon the upregulation of CaM-dependent pathways, need not involve classical inflammatory pathways involving NFκB and indicate that high levels of irradiation may activate a proapoptotic NFκB-mediated pathway in macrophages (*39*).

Mass Spectrometry Detects Limited Protein Abundance Changes of Cellular Proteins Following Irradiation. To determine the specificity of observed changes in CaM abundance relative to other cellular proteins, we have used quantitative mass spectrometry to assess possible changes in expression levels of macrophage proteins. Cellular lysates were prepared and subjected to trypsin digestion, and samples were isotopically labeled prior to LC separation and mass spectrometric analysis of matched samples to permit a quantitative measurement of protein abundance changes (see Figure S3 in the Supporting Information). Between 245 and 800 matched peptide pairs were identified per treatment. We find that the abundances of less than 7% of the observed peptide pairs change following irradiation (Table 1). In all cases, the observed abundance changes are substantially larger than the 1% change in peptide abundances observed upon comparison of the proteomes of wild-type macrophages and those expressing an empty vector. Only 3% of the observed peptide pairs undergo significant abundance changes following the overexpression of CaM. However, the relatively small changes in the abundance of cellular proteins is in marked contrast to prior findings of large and dramatic differences in the proteome of macrophages as part of the host response to bacterial activation (*40*). These measurements indicate that cellular irradiation (i.e., 1 Gy) results in targeted changes in the proteome that involve a relatively small subset of cellular proteins. Further, the overexpression of CaM results in less abundance changes than radiation treatment (i.e., 3 and 7%, respectively) (Table 1).

Diminished Radiation-Induced Cell Death upon CaM Overexpression. Altering CaM levels and NFκB-dependent pathways will have multiple effects, some of which may disrupt DNA damage response pathways and cellular apoptosis (*41*). To identify whether the mechanisms underlying increases in

Table 1. Global Proteomic Measurements of RAW 264.7 Macrophages[a]

	transfection controls		1 Gy radiation		
isotopic labeling ratio ($^{16}O/^{18}O$)	empty vector, WT/WT^{EV}	CaM vector, CaM/WT^{EV}	radiation, WT/WT 1 Gy	radiation, CaM /CaM 1 Gy	CaM vector, WT^{EV}1 Gy/CaM 1 Gy
identified peptide pairs	800	363	245	785	662
differentially expressed peptides	7 (1%)	9 (3%)	17 (7%)	23 (3%)	27 (4%)
identified proteins	480	228	188	457	392
DNA repair pathways	4	1	5	6	5
CaM binding partners	6	1	1	3	3
calcium binding/signaling	24	15	10	23	21
cytokine activation	9	4	4	10	5
cellular communication	6	6	1	6	7
oxidative stress	1	2	2	1	5
differentially expressed proteins	0	0	0	1	2

[a] The column heads give the following information: variable, isotopic labeling ($^{16}O/^{18}O$). Macrophage protein extracts were subjected to tryptic digestion followed by isotopic labeling using either $H_2{}^{16}O$ or $H_2{}^{18}O$ (95%, Sigma-Aldrich) and were then mixed (1:1 ratio by mass) as indicated and analyzed using a capillary LC system coupled online with a hybrid LTQ-Orbitrap mass spectrometer for pairwise comparisons by LC−MS (*30*), where samples correspond to wild-type (WT) cells, macrophages transfected with an empty vector control (WT^{EV}), or macrophages overexpressing a 2-fold molar excess of CaM (CaM), as fully described in the Experimental Procedures. When indicated, the cells were exposed to 1 Gy of X-ray irradiation. Selected identified proteins are indicated in the Supporting Information (Table S1).

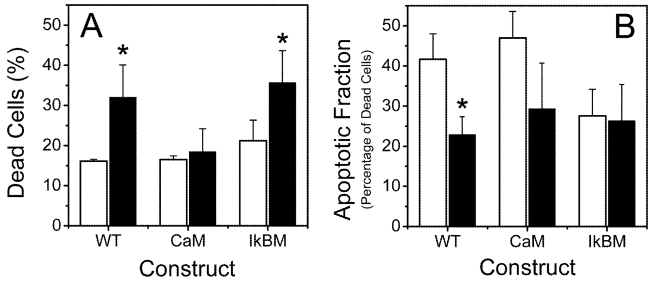

Figure 3. CaM overexpression reduces radiation-dependent cell killing. The viability of individual cells was determined prior to (open bars) or 1 h following (black bars) 1 Gy of irradiation for wild-type RAW 264.7 macrophages (WT) or macrophages overexpressing CaM or the dominant-negative IκBM construct. The panels depict radiation-induced changes in dead cells (A) and the fraction of dead cells that are undergoing apoptosis (B). Dead cells were measured as the fraction of cells stained with propidium iodide relative to the total number of stained cells detected using Hoeschst 33342, while apoptotic cells represent dead cells with condensed nuclei, where nuclear condensation provides a measure of macrophages committed to cellular apoptosis. Indicated values represent the average of three experiments and the associated standard errors of the mean, where more than 250 cells were assessed for each measurement. The asterisk indicates statistical significance ($p < 0.05$) relative to the untreated control.

clonogenic survival one week following irradiation are consistent with cell survival immediately following radiation, we have measured viability at the level of individual cells at early times (i.e., 1 h postirradiation). The DNA intercalating dyes propidium iodide and Hoeschst 33342 stain were used to measure the fraction of dead cells relative to total cells, respectively. Further, on the basis of the presence of condensed nuclei in propidium iodide-stained cells, the fraction of dead cells that are initiating apoptosis was determined. Consistent with our measurements of clonogenic survival, we find a significant increase in the number of dead cells that take up propidium iodide following exposure of wild-type macrophages to 1 Gy of radiation (Figure 3A). Cell death occurs largely by a nonapoptotic means, presumably as necrosis, since the fraction of dead wild-type cells that undergo apoptosis declines following irradiation (Figure 3B). Consistent with results obtained from assays of clonogenic survival, radiation-induced cell death at early times (i.e., 1 h) is substantially diminished by the expression of a 2-fold increase in cellular CaM abundance (Figure 3A). There are similar decreases in the fraction of dead cells that have undergone apoptosis in both wild-type macrophages and cells expressing the CaM construct, suggesting that the mechanism of radiation-induced cell death at this early time (i.e., 1 h following exposure) does not involve apoptosis. In comparison, the selective inhibition of NFκB-dependent nuclear activation does not affect the radiosensitivity of this construct relative to wild-type macrophages (Figure 3A). The fraction of cells undergoing apoptosis upon inhibition of NFκB-dependent pathways, prior to irradiation is less than that of the wild type and is unaffected by radiation (Figure 3B). These results emphasize that increases in clonogenic survival upon inhibition of NFκB-dependent pathways, which involve decreases in rates of apoptosis, are distinct from those involving CaM overexpression (Figures 2 and 3).

CaM Overexpression Disrupts Adaptive Cellular Responses to Low-Dose Radiation. Exposures to low priming doses of radiation (e.g., 0.05 Gy) enhance the radioresistance of virtually all eukaryotic cell lines to a subsequent high-dose exposure (*42*). Similar adaptive responses are apparent in hematopoietic cells from irradiated mice (*43*) or following preconditioning treatments involving an oxidative stress (e.g., hypoxia and reperfusion) (*44, 45*). As the adaptive response to irradiation is abolished with inhibition of NFκB or protein kinase C (PKC), where PKC inhibition results from increases in CaM abundance (*42, 46, 47*), the adaptive response provides a means to assess the possible cross-talk between NFκB- and CaM-dependent pathways. We have therefore assessed the adaptive response in macrophages, comparing the clonogenic survival of wild-type macrophages with stable cell lines either overexpressing CaM or following inhibition of NFκB-dependent pathways.

In wild-type macrophages we observe the classic adaptive response, where prior exposure to low-dose radiation enhances clonogenic survival as compared with that of unprimed controls, resulting in an enhanced number of colonies at each radiation dose (Figure 4A). Following low-dose exposures, the effective dose of radiation associated with 50% cell killing increases from 0.5 to 1.3 Gy for the wild-type cells. As expected from prior measurements (*47*), inhibition of NFκB-dependent pathways results in a radioresistance similar to that of unprimed wild-type cells, largely abolishing the adaptive cellular responses to radiation (Figure 4C). Likewise, the overexpression of CaM abolishes the adaptive cellular responses to radiation (Figure 4B). These results indicate that general inflammatory pathways involving NFκB activation and specific pathways sensitive to changes in CaM abundance (e.g., PKC) act to modulate the radiosensitivities of macrophages through different mechanisms.

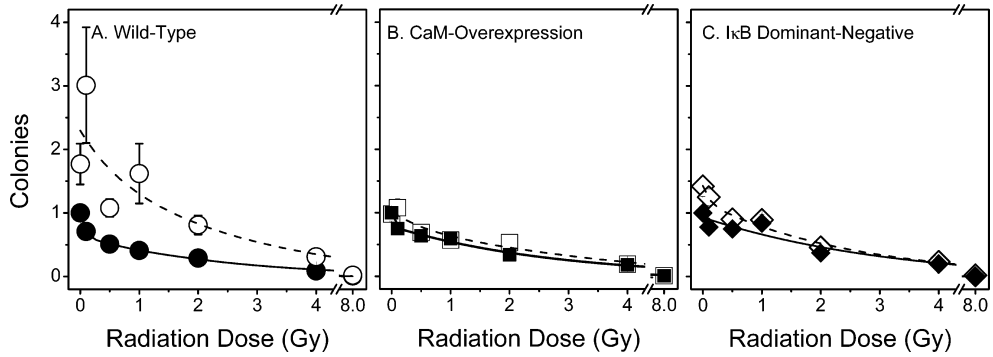

Figure 4. Adaptive cellular responses to low-dose radiation exposure. Dose dependencies of clonogenic survival for wild-type RAW 264.7 macrophages (A) and cells stably overexpressing CaM (B) or the IκB dominant-negative construct (C) before (closed symbols) and following (open symbols) prior exposure to low doses (i.e., 0.05 Gy) of radiation. In all cases, low-dose radiation treatments were carried out 4 h prior to the challenge dose. Indicated values represent the average of six independent measurements and the associated standard errors of the mean. Experimental conditions are as described in the caption to Figure 2.

Radiation-Induced DNA Damage Is Insensitive to CaM. In an attempt to understand the molecular basis for the sensitivity of macrophages to low therapeutic doses of ionizing radiation, we have investigated the possible role of CaM in modulating double-stranded DNA damage, which has been suggested to represent a principle mechanism associated with radiation-induced cellular death and transformation (*48*). In this respect, prior measurements have demonstrated that CaM and histone H2AX interact to form a protein complex that dissociates upon cellular exposure to high doses of radiation (*13*), suggesting a possible functional involvement for CaM in promoting DNA repair. Alternatively, CaM may act to diminish rates of DNA damage through a variety of mechanisms that either reduce rates of reactive oxygen species generation or act to promote alterations in chromatin structure to diminish the sensitivity of DNA to oxidative damage (*7, 49, 50*).

DNA damage was measured using a modified Comet assay, which uses buffer conditions and a dye that selectively intercalates into double-stranded DNA to eliminate the detection of single-stranded DNA breaks, permitting the selective measurement of double-stranded DNA breaks (*26*). This assay measures increases in the mobility of the DNA tail length in an electric field. Prior to irradiation the nucleoids of wild-type macrophages and cells overexpressing CaM and a dominant-negative IκB construct (IκBM) are all of a similar size, and there is no evidence of DNA fragmentation (Figure 5A). Following 1 Gy of irradiation, there are time-dependent increases in the Comet tail length, which overall increases to approximately 15 μm irrespective of the overexpression of CaM or selective inhibition of NFκB-dependent inflammatory pathways (Figure 5B). Substantial DNA damage is detected 4 h following irradiation. In comparison, we detect minimal DNA damage at short times, including 30 min following exposure to low-dose (1 Gy) radiation. These results are in contrast to substantial DNA damage apparent following exposure to high-dose (e.g., 80 Gy) irradiation that is apparent in minutes following exposure (*28*). Thus, there is a substantial lag between irradiation with 1 Gy and the appearance of substantial double-stranded DNA damage using the Comet assay (i.e., >30 min). This observation reflects that much of the damage resulting from low doses of irradiation is due to an indirect mechanism associated with increases in reactive cellular metabolites, which is consistent with prior measurements that demonstrate increased radical formation from leaking mitochondria following cellular irradiation (*51*).

The kinetics of DNA damage from irradiation is very similar for wild-type macrophages and constructs overexpressing CaM

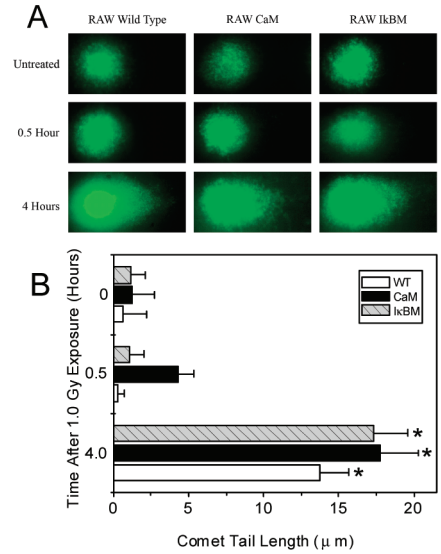

Figure 5. Detection of DNA damage. (A) Representative images illustrating detection of double-stranded DNA breaks using the Comet assay to measure the tail length as the increased mobility of double-stranded DNA fragments (stained with SYBER Green I) outside the nucleoid body following electrophoretic separation in an electric field (1.0 V/cm for 10 min). (B) Quantitation for (i) wild-type RAW 264.7 macrophages (open bars) and cells overexpressing (ii) CaM (black bars) or (iii) the IκB dominant-negative construct (gray striped bars) at indicated times following 1 Gy of radiation exposure. Indicated values represent the average of 26 measurements of individual nucleoids and the associated standard errors of the mean for each experimental condition. The asterisk indicates statistical significance ($p < 0.05$) relative to the untreated control.

or IκBM. The increase in the Comet tail length upon exposure to 1 Gy of radiation is consistent with prior measurements that detect increases in double-stranded DNA breaks in response to a range of other physiologically relevant cellular challenges (*52*). The insensitivity of radiation-induced DNA damage to changes in CaM abundance or NFκB-dependent inflammatory pathways to low-dose irradiation indicates that changes in cellular viability for macrophage constructs overexpressing CaM or involving the targeted inhibition of NFκB pathways are unrelated to the formation of double-strand DNA breaks. These latter results are consistent with prior measurements indicating the promotion of DNA repair pathways in response to ionizing radiation play a primary role in mediating cellular survival (*28*).

Likewise, similar levels of DNA damage are apparent for wild-type macrophages and those overexpressing CaM at higher doses of radiation (i.e., 5 Gy) where less than 20% of macrophages survive irradiation (Figure S1C,D in the Support-

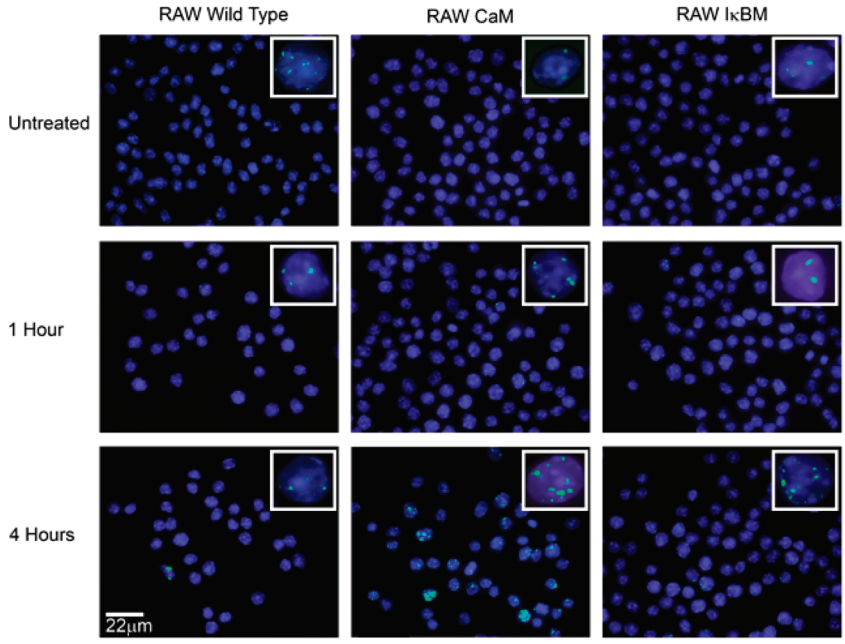

Figure 6. Resolution of DNA repair complexes involving histone γH2AX. Image of fields of fixed and permeabilized wild-type RAW 264.7 macrophages (left panels) and cells overexpressing CaM (middle panels) or the IκB dominant-negative construct (right panels) detected without (top row) and 1 h (middle row) or 4 h (bottom row) after exposure to 1 Gy of X-ray radiation. The insets in the top right corners of each panel show selected nuclei with foci to permit better visualization. Bright green spots correspond to foci detected using antibodies against phosphorylated histone H2AX (i.e., γH2AX) associated with the DNA repair complex within DAPI-stained nuclei (blue).

ing Information). In comparison, at high radiation doses there are large increases in the Comet tail length upon inhibition of NFκB-dependent pathways due to decreased rates of apoptosis (Figure 3B), which result in an accumulation of adherent cells with larger amounts of DNA damage (Figure S1D). These latter results further emphasize that CaM-dependent pathways associated with radioresistance are distinct from those involving the NFκB-dependent pathway. Furthermore, this suggests that no meaningful conclusions can be drawn at high radiation doses, regarding possible differences in macrophage response pathways, due to the substantial loss of viable cells when apoptotic pathways are functional.

CaM-Dependent Activation of DNA Repair Pathways. The possible role of CaM in modulating DNA repair pathways was assessed using immunostaining of adherent macrophages to detect the formation of phosphorylated histone H2AX (γH2AX). γH2AX is associated with double-stranded DNA breaks in euchromatin and acts to recruit protein complexes, which are critical to nonhomologous end-joining and homologous recombination repair pathways (*28, 48*). In response to ionizing radiation, DNA damage occurs in clusters (i.e., foci) (*53*), and the rapid phosphorylation of histone H2AX acts to promote the recruitment of a large number of proteins to sites of double-stranded DNA damage, including Rad50, Rad51, and Brca1 (*13, 28*). We specifically identify these radiation-induced foci, which are larger than 50 000 nm^2 and are distinct from the extremely small foci (i.e., <200 nm^2) that have previously been identified during G1 and prophase as part of the normal cell cycle in some cell types (*54*). Further, our measurements exclude mitotic cells (i.e., nonadherent macrophages) and involve hematopoietic derived cells where this cell cycle specific staining against γH2AX does not occur (*55*). We emphasize that the formation of histone γH2AX foci represents the initiation of DNA repair pathways that can be modulated by a critical signal transduction protein (i.e., CaM) and thus does not necessarily correlate with the extent of DNA damage (*17*).

In wild-type RAW 264.7 macrophages, we find that following irradiation with 1 Gy of X-rays that there are small increases

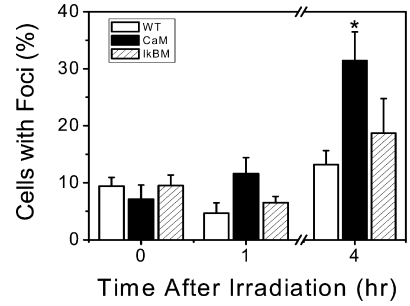

Figure 7. Enhanced DNA repair following up-regulation of CaM abundance. Average number of cells with visible foci containing γH2AX repair complexes in wild-type RAW 264.7 macrophages (open bars) and in macrophage stable cell lines overexpressing CaM (black bars) or an IκB dominant-negative construct (striped bars). Experimental conditions are as described in the caption to Figure 6. Errors represent the standard errors of the mean for two (untreated) or ten (treated) independent measurements, where each measurement interrogated more than 60 nuclei. The asterisk indicates statistical significance ($p < 0.05$) relative to the untreated control.

in the fraction of cells with measurable foci of γH2AX repair complexes (Figure 6). Prior to irradiation, we observe that approximately 9 ± 2% of all cells exhibit foci visible using antibodies against γH2AX (Figure 7). Four hours following irradiation, the number of foci in wild-type macrophages increases to 13 ± 2% of all cells (Figure 7). The minimal sensitivity of histone γH2AX-mediated DNA repair foci to these therapeutic doses of radiation is consistent with earlier suggestions that there is a threshold amount of damage required to initiate DNA repair pathways (*5, 56*). Consistent with this concept, at high doses of radiation (i.e., 5 Gy) 48 ± 5% of wild-type macrophage nuclei are histone γH2AX positive (Figure S2 in the Supporting Information).

In untreated control cells overexpressing CaM or IκBM, there are minimal numbers of γH2AX positive cells, which is consistent with that observed in wild-type cells (Figures 6 and 7). In comparison, following irradiation there are large increases in the percentage of cells that exhibit γH2AX foci (i.e., repair

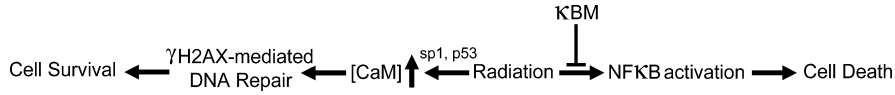

Figure 8. Alternate pathways enhance cellular survival in response to ionizing radiation. Increases in cellular survival following radiation exposures and the formation of reactive oxygen species (ROS) associated with double-stranded DNA damage are enhanced by (i) specific CaM-dependent pathways involving histone H2AX phosphorylation (i.e., formation of γH2AX) to promote DNA repair or (ii) inhibition of nonspecific inflammatory pathways involving NFκB-mediated apoptosis by the overexpression of the dominant-negative IkB construct deficient in sites of phosphorylation (IkBM). Radiation-dependent increases in CaM abundance involve activation of transcription factors Sp1 and p53, known to undergo rapid nuclear translocation in response to radiation exposure. Sp1 is the only transcription factor known to up-regulate CaM expression (*63, 66*), whereas the upstream promoter of CaM genes contains a putative binding site for p53.

complexes) in cells overexpressing CaM (Figure 6), which increases from 7 ± 2% to 31 ± 5% of the cellular population 4 h following irradiation (Figure 7). Similarly CaM-dependent increases in γH2AX foci are present at increased levels (i.e., 85 ± 6%) with higher radiation doses (i.e., 5 Gy) (Figure S2 in the Supporting Information). These measurements strongly indicate a role for CaM in specifically promoting the increased radioresistance of macrophages through the promotion of γH2AX-mediated DNA repair pathways. Activation of H2AX-mediated DNA repair pathways via CaM-dependent mechanisms are independent of meeting a threshold of DNA damage, as previously suggested (*5*). In contrast to these results, there are no statistically significant increases in the number of foci associated with histone γH2AX repair complexes following inhibition of NFκB pathways in IκBM cells in comparison to wild-type macrophages (Figures 6 and 7). Thus, increases in cellular radioresistance upon inhibition of NFκB pathways act through alternative pathways associated with a diminished sensitivity to cellular apoptosis (Figure 3) and do not involve the modulation of γH2AX-mediated DNA repair pathways. In conclusion, our results demonstrate the activation of a CaM-dependent pathway that is associated with phosphorylation of H2AX bound to chromatin. Since phosphorylated H2AX is well recognized to be "an important step in recruiting and maintaining" factors associated with DNA repair (*17*), our results demonstrate an important and previously unrecognized role for CaM in promoting the activation of the DNA repair pathway involving phosphorylated H2AX (*13, 28*), that is independent of DNA damage.

Transient or sustained increases in CaM abundance may affect the cellular phenotype to promote radioresistance through multiple pathways that involve the recruitment of different binding partners to chromatin through the formation of foci enriched in γH2AX that acts to recruit DNA repair proteins. Our data of a CaM-dependent pathway are important, as there is some "confusion when it comes to the identity of the kinase(s) that phosphorylates H2AX in response to IR-induced double stranded breaks", which need not involve the dominant role of ATR as "being the primary kinase responsible for H2AX phoshorylation in response to replicative stress and UV radiation" (*57*). These results, furthermore, are consistent with a recent report in *Science* by Soutoglou and Misteli demonstrating "an activation of the cellular DNA damage response in the absence of DNA lesions" (*17*). Thus, the up-regulation of CaM-dependent pathways promotes the formation of γH2AX foci when DNA damage remains constant, emphasizing a role for CaM in a parallel activation pathway that initiates the formation of the central DNA repair complex involving H2AX (*28*).

Discussion

Exposure to ionizing radiation induces a dose-dependent increase in CaM abundance in RAW 264.7 macrophages (Figure 1). In contrast, irradiation at doses associated with (i) a large 6-fold increase in CaM abundance and (ii) a 3-fold increases in foci containing phosphorylated histone H2AX does not result in large-scale changes in the macrophage proteome (Table 1, Figure S3 in the Supporting Information). Increases in CaM abundance are found to diminish the radiosensitivity of macrophages (Figures 2 and 3A). Increases in CaM abundance have no effect on the sensitivity of macrophages to radiation-induced double-stranded DNA damage (Figure 5), indicating that CaM-dependent pathways do not alter chromatin structure to modulate the sensitivity of genomic DNA to radiation-induced damage. Likewise, CaM-dependent increases in radioresistance are unrelated to apoptotic pathways involving NFκB (Figure 3B). Thus, CaM-dependent response pathways synergize with repair pathways activated directly by DNA damage to increase levels of histone H2AX phosphorylation (Figures 6 and 7). The ability of CaM-dependent pathways to promote histone H2AX phosphorylation, which in turn mediates the recruitment of DNA repair proteins to sites of damage, enhances macrophage survival upon cellular irradiation (Figure 8).

CaM binding to cytoskeletal networks has long been linked to tumoricidal activities in macrophages, while increases in CaM abundance are associated with cell transformation in general (*58, 59*). Our results indicate that CaM plays additional roles in the maintenance of cell viability in response to radiation exposure through the up-regulation of γH2AX-dependent DNA repair pathways (Figures 1, 3, 6, and 7). Consistent with our observations, prior measurements have (i) identified a physical association between CaM and histone H2AX that is altered by radiation exposure (*12*) and (ii) demonstrated that CaM can promote the phosphorylation of histone H2AX through the activation of protein kinase DNA-PK, which is known to play a critical role in mediating double-stranded DNA repair through nonhomologous end-joining mechanisms (*13, 60, 61*). As phosphorylated histone H2AX acts as an organizing center to anchor chromosomal ends to mediate DNA repair (*13, 48*), these results have a broad significance with respect to understanding the mechanisms of radioresistance for macrophages and other hematopoietic cell types in response to radiation exposure.

The up-regulation of CaM-dependent DNA repair pathways is augmented by the accumulation of DNA damage (Figure 5). Thus, the modulation of CaM abundance acts to enhance the sensitivity of the H2AX-mediated DNA repair pathways to radiation-induced double-stranded DNA breaks, thereby reducing low-dose radiation hypersensitivity. These results indicate that the activation of H2AX-dependent pathways is not dependent upon a minimum threshold of DNA damage. In keeping with our findings that CaM overexpression increases the number of foci containing H2AX DNA repair complexes after irradiation (Figure 6), others have found that CaM antagonists fully or partially block double-stranded DNA repair (*62, 63*). These results are consistent with the known linkage between CaM-dependent pathways and the activation of multiple kinases, including Akt and DNA-PK, which are known to be critical to histone H2AX phoshorylation and DNA repair (*61*). Our finding that CaM plays a central role in mediating macrophage

radioresistance therefore supports prior suggestions that CaM represents an effective therapeutic target in conjunction with radiotherapies (*64*).

Increases in CaM abundance in response to radiation exposure are consistent with the promoter structures of all three CaM genes, which contain binding sites for transcription factors Sp1 and p53; both of these transcription factors are known to be activated in response to clinically relevant radiation exposures (i.e., <2 Gy) (*65*−*67*). Further, the sensitivity of Sp1 and p53 to radiation exposure is consistent with observed increases in CaM abundance upon irradiation (Figure 1). Our findings that double-stranded DNA damage resulting from low (therapeutic) levels of ionizing radiation is a target for repair through the up-regulation of CaM-dependent pathways that promote phosphorylation of histone H2AX, which is critical for DNA repair complex assembly, are consistent with a functional role for these transcription factors in mediating cellular responses to ionizing radiation (Figure 8).

Prior exposure of macrophages, and other cell types, to low priming doses of radiation initiates an adaptive response (i.e., preconditioning) that enhances cell survival to subsequent higher doses of radiation (Figures 1 and 4A) (*68, 69*). This adaptive response is abolished when the priming radiation dose increases above 0.5 Gy (*69*), which is commonly interpreted to suggest that fundamentally distinct cellular mechanisms are associated with responses to low and high radiation doses (*34, 35*). Alternatively, radiation-dependent increases in the abundance of key regulators such as CaM (Figure 1), whose overall concentration limits the activation of many cellular proteins (*70*), have the potential to act as a switching mechanism to differentially activate cellular pathways in response to radiation doses. Indeed, it is well understood that the mobilization of CaM in response to calcium transients acts to regulate NFAT-dependent gene transcription through the differential binding between CaM and protein phosphatases (e.g., calcineurin) and kinases (e.g., CaM-dependent protein kinase) (*71*). A similar type of regulation may occur in macrophages, where increases in CaM abundance in response to a single dose of ionizing radiation act to enhance DNA repair pathways involving γH2AX by changing the balance between phosphatase and kinase activities to reduce the hypersensitivity of macrophages to low levels of radiation (Figures 1B, 6, and 7). Inhibition of the adaptive response upon large increases in CaM abundance, resulting from 2-fold overexpression or a priming dose of radiation, may be the result of the activation of alternative CaM-dependent pathways (Figure 4B). For example, PKC activity is required for the adaptive response and is inhibited by CaM association (*42, 46*). Likewise, inhibition of the adaptive response at priming doses of radiation above 0.5 Gy may arise due to increases in CaM levels, which act to inhibit PKC activity and which in macrophages increase by more than 4-fold (Figure 1). Thus, the relative amount of CaM and target proteins is likely to contribute to an integrated cellular response to radiation exposure.

In conclusion, we have demonstrated that increases in CaM abundance in response to radiation exposure, enhance macrophage survival through pathways involving the phosphorylation of histone H2AX, which is required for both nonhomologous end-joining and homologous DNA repair pathways. This pathway, involving CaM and histone H2AX, is distinct from NFκB pathways that act to enhance cellular apoptosis in response to radiation. These results suggest that therapeutic treatments that target CaM may be of considerable efficacy in conjunction with traditional radiotherapies to promote the killing of tumor-associated macrophages and are likely to have other beneficial effects as CaM antagonists are known to prevent cancer invasiveness (*58*). Future measurements will need to identify the components of the CaM-dependent pathway that leads to histone H2AX phosphorylation, thereby activating DNA repair and enhancing macrophage survival following radiation exposure.

Acknowledgment. This work was completed as part of the student radiobiology laboratory associated with course ES/RP 416/516 at Washington State University Tri-Cites, Richland, WA. P.E.E. and D.J.W. are students in the Environmental Sciences Program at Washington State University Tri-Cities. H.S.S. and T.C.S. have joint appointments with Washington State University Tri-Cities and Pacific Northwest National Laboratory (PNNL). A portion of the research was performed using EMSL, a national scientific user facility sponsored by the Department of Energy's Office of Biological and Environmental Research located at Pacific Northwest National Laboratory. We thank Diana J. Bigelow, Antone L. Brooks, Allan S. Felsot, and James E. Morris for insightful discussions, William B. Chrisler, Sue Karagiosis, Sewite Negash, David L. Stenoien, Colette A. Sacksteder, and Katrina Walters for technical assistance, Banu Gopalan for her analysis of CaM promoter structures, and class members Inna Berezovsky, Holly Bowers, Matthew Call, Wanda Elliott, Enid Flynn, Jesse Lamb, Chandra Lindberg, Travis Schuller, Galina York, and Meg Mercer of Radiation Biology ES/RP 416/516 for their participation in data collection.

Supporting Information Available: Additional data regarding protein abundance changes visualized using immunoblots or obtained using mass spectrometry as well as dose-dependent data relating to cell survival, DNA damage, and the formation of foci enriched in histone γH2AX. This material is available free of charge via the Internet at http://pubs.acs.org.

References

(1) Torroella-Kouri, M., Ma, X., Perry, G., Ivanova, M., Cejas, P. J., Owen, J. L., Iragavarapu-Charyulu, V., and Lopez, D. M. (2005) Diminished expression of transcription factors nuclear factor kappaB and CCAAT/enhancer binding protein underlies a novel tumor evasion mechanism affecting macrophages of mammary tumor-bearing mice. *Cancer Res. 65*, 10578–10584.

(2) Mantovani, A., Schioppa, T., Porta, C., Allavena, P., and Sica, A. (2006) Role of tumor-associated macrophages in tumor progression and invasion. *Cancer Metastasis Rev. 25*, 315–322.

(3) Perkins, E. H., Nettesheim, P., and Morita, T. (1966) Radioresistance of the engulfing and degradative capacities of peritoneal phagocytes to kiloroentgen x-ray doses. *J. Reticuloendothel. Soc. 3*, 71–82.

(4) Wu, J. T., and Kral, J. G. (2005) The NF-kappaB/IkappaB signaling system: a molecular target in breast cancer therapy. *J. Surg. Res. 123*, 158–169.

(5) Marples, B., Wouters, B. G., Collis, S. J., Chalmers, A. J., and Joiner, M. C. (2004) Low-dose hyper-radiosensitivity: a consequence of ineffective cell cycle arrest of radiation-damaged G2-phase cells. *Radiat. Res. 161*, 247–255.

(6) Hildebrandt, G., Seed, M. P., Freemantle, C. N., Alam, C. A., Colville-Nash, P. R., and Trott, K. R. (1998) Mechanisms of the anti-inflammatory activity of low-dose radiation therapy. *Int. J. Radiat. Biol. 74*, 367–378.

(7) Smallwood, H. S., Shi, L., and Squier, T. C. (2006) Increases in calmodulin abundance and stabilization of activated inducible nitric oxide synthase mediate bacterial killing in RAW 264.7 macrophages. *Biochemistry 45*, 9717–9726.

(8) Clapham, D. E. (2007) Calcium signaling. *Cell 131*, 1047–1058.

(9) Yap, K. L., Kim, J., Truong, K., Sherman, M., Yuan, T., and Ikura, M. (2000) Calmodulin target database. *J. Struct. Funct. Genomics 1*, 8–14.

(10) Haghighat, N., and Al-Hashimi, I. (1999) A pilot study on the effect of radiation on calmodulin in rat submandibular salivary glands. *Arch. Oral Biol. 44*, 383–389.

(11) Takagi, A., and Iizuka, H. (1995) UVB-induced calmodulin increase in pig epidermis: Analysis of the effect of the calmodulin antagonist, W-13. *Arch. Dermatol. Res. 287*, 326–332.
(12) Du, Y. C., Gu, S., Zhou, J., Wang, T., Cai, H., Macinnes, M. A., Bradbury, E. M., and Chen, X. (2006) The dynamic alterations of H2AX complex during DNA repair detected by a proteomic approach reveal the critical roles of Ca(2+)/calmodulin in the ionizing radiation-induced cell cycle arrest. *Mol. Cell. Proteomics 5*, 1033–1044.
(13) Foster, E. R., and Downs, J. A. (2005) Histone H2A phosphorylation in DNA double-strand break repair. *FEBS J. 272*, 3231–3240.
(14) Redon, C., Pilch, D., Rogakou, E., Sedelnikova, O., Newrock, K., and Bonner, W. (2002) Histone H2A variants H2AX and H2AZ. *Curr. Opin. Genet. Dev. 12*, 162–169.
(15) Cowell, I. G., Sunter, N. J., Singh, P. B., Austin, C. A., Durkacz, B. W., and Tilby, M. J. (2007) gammaH2AX foci form preferentially in euchromatin after ionising-radiation. *PLoS ONE 2*, e1057.
(16) Tanaka, T., Huang, X., Halicka, H. D., Zhao, H., Traganos, F., Albino, A. P., Dai, W., and Darzynkiewicz, Z. (2007) Cytometry of ATM activation and histone H2AX phosphorylation to estimate extent of DNA damage induced by exogenous agents. *Cytometry A 71*, 648–661.
(17) Soutoglou, E., and Misteli, T. (2008) Activation of the cellular DNA damage response in the absence of DNA lesions. *Science 320*, 1507–1510.
(18) Hall, E. (2000) *Radiobiology for the Radiologist*, 5th ed., Harper and Row, Hagerstown, MD.
(19) Cao, J., Liu, Y., Jia, L., Zhou, H. M., Kong, Y., Yang, G., Jiang, L. P., Li, Q. J., and Zhong, L. F. (2007) Curcumin induces apoptosis through mitochondrial hyperpolarization and mtDNA damage in human hepatoma G2 cells. *Free Radical Biol. Med. 43*, 968–975.
(20) Florea, A. M., and Busselberg, D. (2008) Arsenic trioxide in environmentally and clinically relevant concentrations interacts with calcium homeostasis and induces cell type specific cell death in tumor and non-tumor cells. *Toxicol. Lett. 179*, 34–42.
(21) Plesca, D., Mazumder, S., and Almasan, A. (2008) Chapter 6 DNA damage response and apoptosis. *Methods Enzymol. 446*, 107–122.
(22) Andreau, K., Castedo, M., Perfettini, J. L., Roumier, T., Pichart, E., Souquere, S., Vivet, S., Larochette, N., and Kroemer, G. (2004) Preapoptotic chromatin condensation upstream of the mitochondrial checkpoint. *J. Biol. Chem. 279*, 55937–55945.
(23) Andreau, K., Perfettini, J. L., Castedo, M., Metivier, D., Scott, V., Pierron, G., and Kroemer, G. (2004) Contagious apoptosis facilitated by the HIV-1 envelope: fusion-induced cell-to-cell transmission of a lethal signal. *J. Cell Sci. 117*, 5643–5653.
(24) Henery, S., George, T., Hall, B., Basiji, D., Ortyn, W., and Morrissey, P. (2008) Quantitative image based apoptotic index measurement using multispectral imaging flow cytometry: A comparison with standard photometric methods. *Apoptosis 13*, 1054–1063.
(25) Yasuhara, S., Zhu, Y., Matsui, T., Tipirneni, N., Yasuhara, Y., Kaneki, M., Rosenzweig, A., and Martyn, J. A. (2003) Comparison of comet assay, electron microscopy, and flow cytometry for detection of apoptosis. *J. Histochem. Cytochem. 51*, 873–885.
(26) Lemay, M., and Wood, K. A. (1999) Detection of DNA damage and identification of UV-induced photoproducts using the CometAssay kit. *Biotechniques 27*, 846–851.
(27) Shrivastav, M., De Haro, L. P., and Nickoloff, J. A. (2008) Regulation of DNA double-strand break repair pathway choice. *Cell Res. 18*, 134–147.
(28) Paull, T. T., Rogakou, E. P., Yamazaki, V., Kirchgessner, C. U., Gellert, M., and Bonner, W. M. (2000) A critical role for histone H2AX in recruitment of repair factors to nuclear foci after DNA damage. *Curr. Biol. 10*, 886–895.
(29) Ferrington, D. A., Yao, Q., Squier, T. C., and Bigelow, D. J. (2002) Comparable levels of Ca-ATPase inhibition by phospholamban in slow-twitch skeletal and cardiac sarcoplasmic reticulum. *Biochemistry 41*, 13289–13296.
(30) Lopez-Ferrer, D., Heibeck, T. H., Petritis, K., Hixson, K. K., Qian, W., Monroe, M. E., Mayampurath, A., Moore, R. J., Belov, M. E., Camp, D. G., 2nd, and and Smith, R. D. (2008) Rapid sample processing for LC-MS-based quantitative proteomics using high intensity focused ultrasound. *J. Proteome Res. 7*, 3860–3867.
(31) Monroe, M. E., Tolic, N., Jaitly, N., Shaw, J. L., Adkins, J. N., and Smith, R. D. (2007) VIPER: An advanced software package to support high-throughput LC-MS peptide identification. *Bioinformatics 23*, 2021–2023.
(32) Smith, R. D. (2002) Advanced mass spectrometric methods for the rapid and quantitative characterization of proteomes. *Comp. Funct. Genomics 3*, 143–150.
(33) Storey, J. D., and Tibshirani, R. (2003) Statistical significance for genomewide studies. *Proc. Natl. Acad. Sci. U.S.A. 100*, 9440–9445.
(34) Brooks, A. L. (2005) Paradigm shifts in radiation biology: Their impact on intervention for radiation-induced disease. *Radiat. Res. 164*, 454–461.
(35) Lambin, P., Malaise, E. P., and Joiner, M. C. (1996) Might intrinsic radioresistance of human tumour cells be induced by radiation? *Int. J. Radiat. Biol. 69*, 279–290.
(36) Verma, S., Xiong, Y., Mayer, M. U., and Squier, T. C. (2007) Remodeling of the bacterial RNA polymerase supramolecular complex in response to environmental conditions. *Biochemistry 46*, 3023–3035.
(37) Weber, T. J., Smallwood, H. S., Kathmann, L. E., Markillie, L. M., Squier, T. C., and Thrall, B. D. (2006) Functional link between TNF biosynthesis and CaM-dependent activation of inducible nitric oxide synthase in RAW 264.7 macrophages. *Am. J. Physiol.: Cell Physiol. 290*, C1512–1520.
(38) Lo, C. J., Garcia, I., Cryer, H. G., and Maier, R. V. (1996) Calcium and calmodulin regulate lipopolysaccharide-induced alveolar macrophage production of tumor necrosis factor and procoagulant activity. *Arch. Surg. 131*, 44–50.
(39) Radhakrishnan, S. K., and Kamalakaran, S. (2006) Pro-apoptotic role of NF-kappaB: Implications for cancer therapy. *Biochim. Biophys. Acta 1766*, 53–62.
(40) Shi, L., Adkins, J. N., Coleman, J. R., Schepmoes, A. A., Dohnkova, A., Mottaz, H. M., Norbeck, A. D., Purvine, S. O., Manes, N. P., Smallwood, H. S., Wang, H., Forbes, J., Gros, P., Uzzau, S., Rodland, K. D., Heffron, F., Smith, R. D., and Squier, T. C. (2006) Proteomic analysis of *Salmonella enterica* serovar Typhimurium isolated from RAW 264.7 macrophages: Identification of a novel protein that contributes to the replication of serovar Typhimurium inside macrophages. *J. Biol. Chem. 281*, 29131–29140.
(41) Ryan, K. M., Ernst, M. K., Rice, N. R., and Vousden, K. H. (2000) Role of NF-kappaB in p53-mediated programmed cell death. *Nature 404*, 892–897.
(42) Shimizu, T., Kato, T., Jr., Tachibana, A., and Sasaki, M. S. (1999) Coordinated regulation of radioadaptive response by protein kinase C and p38 mitogen-activated protein kinase. *Exp. Cell Res. 251*, 424–432.
(43) Wang, G. J., and Cai, L. (2000) Induction of cell-proliferation hormesis and cell-survival adaptive response in mouse hematopoietic cells by whole-body low-dose radiation. *Toxicol. Sci. 53*, 369–376.
(44) Barnett, M. E., Madgwick, D. K., and Takemoto, D. J. (2007) Protein kinase C as a stress sensor. *Cell. Signalling 19*, 1820–1829.
(45) Pespeni, M., Hodnett, M., and Pittet, J. F. (2005) In vivo stress preconditioning. *Methods (San Diego) 35*, 158–164.
(46) Kruger, H., Schroder, W., Buchner, K., and Hucho, F. (1990) Protein kinase C inhibition by calmodulin and its fragments. *J. Protein Chem. 9*, 467–473.
(47) Fan, M., Ahmed, K. M., Coleman, M. C., Spitz, D. R., and Li, J. J. (2007) Nuclear factor-kappaB and manganese superoxide dismutase mediate adaptive radioresistance in low-dose irradiated mouse skin epithelial cells. *Cancer Res. 67*, 3220–3228.
(48) Bassing, C. H., and Alt, F. W. (2004) H2AX may function as an anchor to hold broken chromosomal DNA ends in close proximity. *Cell Cycle 3*, 149–153.
(49) Pirrotta, V. (2004) The ways of PARP. *Cell 119*, 735–736.
(50) Smith, P. J., Mircheva, J., and Bleehen, N. M. (1986) Interaction of bleomycin, hyperthermia and a calmodulin inhibitor (trifluoperazine) in mouse tumour cells: II. DNA damage, repair and chromatin changes. *Br. J. Cancer 53*, 105–114.
(51) Mikkelsen, R. B., and Wardman, P. (2003) Biological chemistry of reactive oxygen and nitrogen and radiation-induced signal transduction mechanisms. *Oncogene 22*, 5734–5754.
(52) Kindzelskii, A. L., and Petty, H. R. (2000) Extremely low frequency pulsed DC electric fields promote neutrophil extension, metabolic resonance and DNA damage when phase-matched with metabolic oscillators. *Biochim. Biophys. Acta 1495*, 90–111.
(53) Purkayastha, S., Milligan, J. R., and Bernhard, W. A. (2007) On the chemical yield of base lesions, strand breaks, and clustered damage generated in plasmid DNA by the direct effect of X rays. *Radiat. Res. 168*, 357–366.
(54) McManus, K. J., and Hendzel, M. J. (2005) ATM-dependent DNA damage-independent mitotic phosphorylation of H2AX in normally growing mammalian cells. *Mol. Biol. Cell 16*, 5013–5025.
(55) Huang, X., Kurose, A., Tanaka, T., Traganos, F., Dai, W., and Darzynkiewicz, Z. (2006) Sequential phosphorylation of Ser-10 on histone H3 and ser-139 on histone H2AX and ATM activation during premature chromosome condensation: relationship to cell-cycle phase and apoptosis. *Cytometry A 69*, 222–229.
(56) Nuta, O. and Darroudi, F. (2008) The impact of the bystander effect on the low-dose hypersensitivity phenomenon. *Radiat. Environ. Biophys. 47*, 265–274.
(57) Stucki, M., and Jackson, S. P. (2006) gammaH2AX and MDC1: Anchoring the DNA-damage-response machinery to broken chromosomes. *DNA Repair 5*, 534–543.
(58) Sherbet, G. (2001) *Calcium Signaling in Cancer*, pp 77−79, CRC Press, Boca Raton, FL.

(59) Mecham, J. O., Soong, M. M., Cain, C. A., Koehm, S., Goff, J., and Tompkins, W. A. (1985) Binding of calmodulin to the microfilament network correlates with induction of a macrophage tumoricidal response. *J. Immunol. 134*, 3516–3523.

(60) Byrum, J., Jordan, S., Safrany, S. T., and Rodgers, W. (2004) Visualization of inositol phosphate-dependent mobility of Ku: Depletion of the DNA-PK cofactor InsP6 inhibits Ku mobility. *Nucleic Acids Res. 32*, 2776–2784.

(61) Reddy, G. P., Barrack, E. R., Dou, Q. P., Menon, M., Pelley, R., Sarkar, F. H., and Sheng, S. (2006) Regulatory processes affecting androgen receptor expression, stability, and function: potential targets to treat hormone-refractory prostate cancer. *J. Cell. Biochem. 98*, 1408–1423.

(62) Herman, M., Ori, Y., Chagnac, A., Weinstein, T., Korzets, A., Zevin, D., Malachi, T., and Gafter, U. (2002) DNA repair in mononuclear cells: role of serine/threonine phosphatases. *J. Lab. Clin. Med. 140*, 255–262.

(63) Wang, Y., Mallya, S. M., and Sikpi, M. O. (2000) Calmodulin antagonists and cAMP inhibit ionizing-radiation-enhancement of double-strand-break repair in human cells. *Mutat. Res. 460*, 29–39.

(64) Seales, E. C., Micoli, K. J., and McDonald, J. M. (2006) Calmodulin is a critical regulator of osteoclastic differentiation, function, and survival. *J. Cell. Biochem. 97*, 45–55.

(65) Raju, U., Gumin, G. J., and Tofilon, P. J. (2000) Radiation-induced transcription factor activation in the rat cerebral cortex. *Int. J. Radiat. Biol. 76*, 1045–1053.

(66) Pan, X., Solomon, S. S., Shah, R. J., Palazzolo, M. R., and Raghow, R. S. (2000) Members of the Sp transcription factor family regulate rat calmodulin gene expression. *J. Lab. Clin. Med. 136*, 157–163.

(67) Criswell, T., Leskov, K., Miyamoto, S., Luo, G., and Boothman, D. A. (2003) Transcription factors activated in mammalian cells after clinically relevant doses of ionizing radiation. *Oncogene 22*, 5813–5827.

(68) Joiner, M. C., Marples, B., Lambin, P., Short, S. C., and Turesson, I. (2001) Low-dose hypersensitivity: current status and possible mechanisms. *Int. J. Radiat. Oncol., Biol., Phys. 49*, 379–389.

(69) Tapio, S., and Jacob, V. (2007) Radioadaptive response revisited. *Radiat. Environ. Biophys. 46*, 1–12.

(70) Tran, Q. K., Black, D. J., and Persechini, A. (2003) Intracellular coupling via limiting calmodulin. *J. Biol. Chem. 278*, 24247–24250.

(71) Bito, H., Deisseroth, K., and Tsien, R. W. (1996) CREB phosphorylation and dephosphorylation: A Ca(2+)- and stimulus duration-dependent switch for hippocampal gene expression. *Cell 87*, 1203–1214.

TX800236R